High-stress abrasion of wear resistant steels in the cutting edges of loader buckets

K. Valtonen[1]*, K. Keltamäki[2], and V.-T. Kuokkala[1]
[1]Tampere University of Technology, Faculty of Engineering Sciences, Laboratory of Materials Science, Tampere Wear Center
P.O. Box 589, FI-33101 Tampere, FINLAND
[2]Lappland University of Applied Sciences, Industry and Natural Resources RDI, Tietokatu 1, FI-94600 Kemi, FINLAND

*Corresponding author: Kati Valtonen, kati.valtonen@tut.fi

Abstract

To simulate the wear behavior of the cutting edge of the mining load-haul-dumper bucket, high-stress abrasion laboratory wear tests were conducted and compared to the in-service tests. The effects of test parameters and different abrasives on the wear rates and wear mechanisms of wear resistant steels were studied using the high-speed slurry-pot with a dry abrasive bed (dry-pot) and in the actual in-service use as a cutting edge. The laboratory wear tests produced results that are well comparable with the in-service case observations. Especially at the higher sample rotation speed with granite as an abrasive, the wear rates were quite similar as determined from the cutting edge of a loader bucket that had been used in a mine.

Keywords: Wear testing; Abrasion; Steel; Mining, mineral processing

1. Introduction

In the mining conditions, it is practically impossible to perform two or more identical wear tests for the cutting edges of the mining loader buckets. Good examples of the variables affecting the results are the different types of rock being loaded, and even the different driving styles of the drivers. During a workday, the loader can be used to load slurry, gravel or large rocks, or simply to scrape the roads clean. The weight of the entire loader concentrates on the cutting edge when the bucket is being filled, especially when the rear tires lift up. Consequently, the cutting edge of the bucket may bend down as much as 50-60 mm [1]. Furthermore, the wear environment and also the mechanical properties of the cutting edge material and the welds affect the lifetime of the cutting edge, which may need to be replaced only once or several times a year.

There are several standardized tests for evaluating the abrasiveness of the rock. The most used ones are the LCPC test (Laboratoires des Ponts et Chaussées, Paris [2]), the Cerchar Abrasivity Index (CAI) test, and the determination of the equivalent quartz content (EQu) from a thin section or using an X-ray diffractometer [3]. In the LCPC test, two steel impellers are rotating five minutes at 4500 rpm in a pot with 500 g of 4-6.3 mm gravel [2]. The limitations of the LCPC test procedure are the quite small amount of abrasives of rather small size, the high rotation speed, and the use of structural steel with low hardness (60-75 HR B [4]) as impellers. In the LCPC tests, quite small differences in the steel properties may have a marked effect on the wear rates that naturally affects directly the obtained abrasiveness values [4,5]. On the other hand, the used steel grade is also quite different from the wear resistant materials used in the mining operations.

The Cerchar Abrasivity Index test is a more controlled test, where the rock samples are scratched with five 55 HRC steel styluses using a 70 kN force [6,7]. Five 10 mm scratches are made on then rock surfaces in two perpendicular directions at the speed of 1 mm/s. The CAI index is determined by measuring the flat area formed in the steel styluses. It has been stated that the CAI index correlates well with the strength [7] and the equivalent quartz content of the rocks [3]. Moreover, its correlation with the LCPC abrasivity index is surprisingly good, when the difference between the test methods is taken into consideration. However, the technique is not suitable for testing of the abrasivity of small particles [3].

In high-stress abrasive wear, so-called white layers can form by a thermomechanical process where the surface temperature during the wear contact first exceeds the austenite formation temperature, followed by a rapid cooling by the underlying bulk metal that leads to the formation of untempered martensite [8–10]. The simultaneous severe plastic deformation can cause the formation of a very fine nanostructure with higher strength and hardness than those of the original surface [14]. In addition, below the white layer the temperature may exceed about 200°C, leading to overtempering of the martensite. The hardness of this so-called dark layer can therefore be markedly lower than the initial hardness of the steel [8]. The formation of both of these layers is frequently observed and studied for example in conjunction of machining experiments [11–16].

The high-speed slurry-pot with a dry abrasive bed (dry-pot) has been successfully used to simulate the wear performance of carbide free bainitic steels in an iron ore sorting machine [17,18]. Moreover, in the comparison of four abrasive and impact abrasive test methods with the in-service mining loader bucket wear behavior, the dry-pot method showed the highest wear rates in heavy abrasive wear conditions [19]. In this article, the dry-pot is also used to study the abrasivity of crushed rock.

This research deals with the effects of test parameters and abrasives on the wear rates and wear mechanisms of steels. High-stress abrasion wear tests were conducted to simulate the wear behavior of the in-service cutting edge of a mining loader in a chromite mine. Six martensitic wear resistant steels of varying hardness were tested using the high-speed slurry-pot equipment with a dry abrasive bed and compared to the in-service cutting-edge steels tested in a chromite mine. The steel samples used in the tests had profiles similar to the actual cutting edges used in the bucket loaders. The abrasives were 8 to 10 mm crushed and sieved particles of quartzite, chromite, and two granites.

2. Materials and methods

2.1 Materials

Six wear resistant steels in the hardness range of 400 HB to 600 HB were wear tested in the laboratory with four abrasives. Table 1 lists the steels and their nominal compositions and typical mechanical properties, including Vickers hardness, yield strength (Rp0.2), ultimate tensile strength (Rm), elongation (A), and impact toughness at -40°C . The typical carbon equivalent values (CEV) were determined using CEV = C + Mn/6 + (Cr + Mo + V)/5 + (Ni + Cu)/15. The microstructure of the studied steels was martensitic with some retained austenite and untempered martensite.

Table 1. Typical mechanical properties and nominal compositions of the tested steels.

	400HB	450HB	R500HB	500HB	550HB	600HB
Hardness [HV10]	401 ± 23	435 ± 6	493 ± 18	481 ± 18	554 ± 8	609 ± 16
Rp0.2 [N/mm^2]	1000	1200	1250	1300	1400	1650
Rm [N/mm^2]	1250	1450	1600	1550	1700	2000
A [%]	10	8	8	8	7	7
Impact toughness -40°C [J]	30	30	30	37	30	20
C [wt%] max.	0.26	0.26	0.30	0.30	0.37	0.47
Si [wt%] max.	0.80	0.80	0.80	0.70	0.50	0.70
Mn [wt%] max.	1.70	1.70	1.7	1.60	1.30	1.4
Cr [wt%] max.	1.5	1.5	1.5	1.5	1.14	1.20
Ni [wt%] max.	1.0	1.0	1.0	1.5	1.4	2.50
Mo [wt%] max.	0.5	0.5	0.5	0.6	0.6	0.70
B [wt%] max.	0.005	0.005	0.005	0.005	0.004	0.005
CEV typical	0.57	0.57	0.66	0.45	0.72	0.61

Swedish quartzite, Finnish chromite, and two granites from Finland were used as abrasives. The initial sieved particle size used in the tests was 8-10 mm. Table 2 lists some properties of the abrasives and Fig. 1 shows their microstructures. The two studied granites have quite similar abrasiveness and crushability, but Kuru granite has a much finer and heterogeneous structure compared to Sorila granite. Moreover, there is a marked difference in their composition; the main constituent in Kuru granite is quartz, while in Sorila granite it is plagioglase (sodium calcium feldspar).

Table 2. Properties and nominal composition of the abrasives.

	Quartzite	Chromite	Kuru granite	Sorila granite
Quarry	Baskarp Svedudden, Sweden	Outokumpu Tornio Works Kemi Mine, Finland	Kuru, Finland	Sorila, Finland
Solid density [t/m^3]	2.65	3.46	2.64	2.72
Crushability [%]	35	79	38	38
Abrasiveness	1940	460	1380	1500
Median hardness [HV1]	992 ± 162	1059 ± 97	977 ± 134	955 ± 159
Nominal mineral contents [%]	Quartz 99	Chromite 99	Quartz 35 Plagioclase 30 Orthoclase 28 Biotite 3 [20]	Plagioclase 45 Quartz 25 Orthoclase 13 Biotite 10 Amphibole 5 [21]

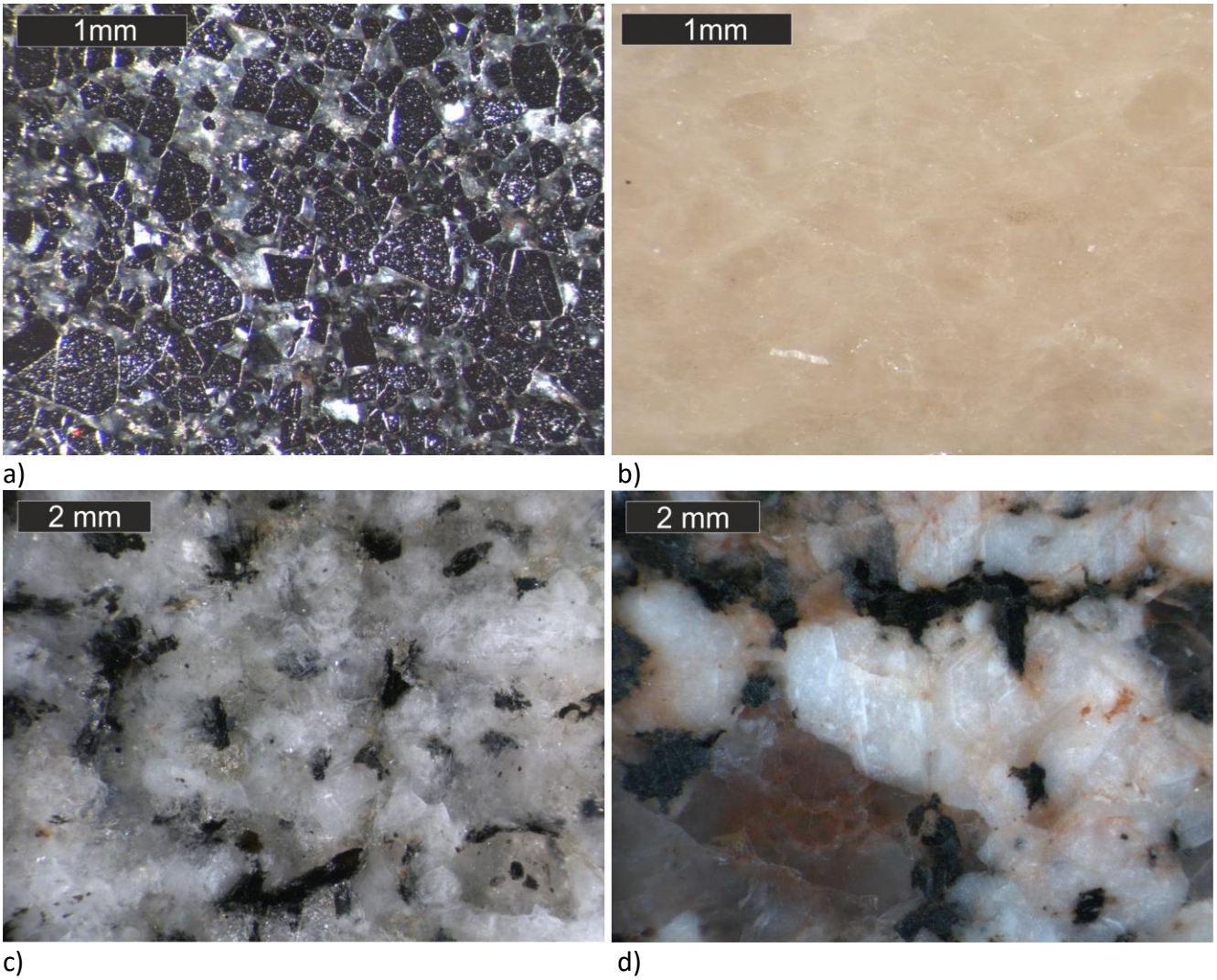

Fig. 1. Stereomicroscope images of the cross-sections of the abrasives: a) chromite, b) quartzite, c) Kuru granite, and d) Sorila granite.

2.2. Methods

Two of the studied steels, R500HB and 550HB were tested also in the in-service mining conditions in Kemi chromite mine. Fig. 2 shows a schematic image of the cutting edge used in an underground mining loader bucket constructed from the above mentioned steels by submerged arc welding (SAW). A CAT R2900G load-haul-dump (LHD) loader was used in normal mine operations for 217 hours, including loading of 51514.6 tons of chromite ore, granite, slurry, and barren rock. The mass loss of the cutting edge of the bucket was determined by ATOS 3D-scanning, which gives three-dimensional measurements of the product for further analysis with Atos software. The wear pattern analysis was made by comparing the 3D scan of an unused cutting edge to the worn cutting edge after the test period.

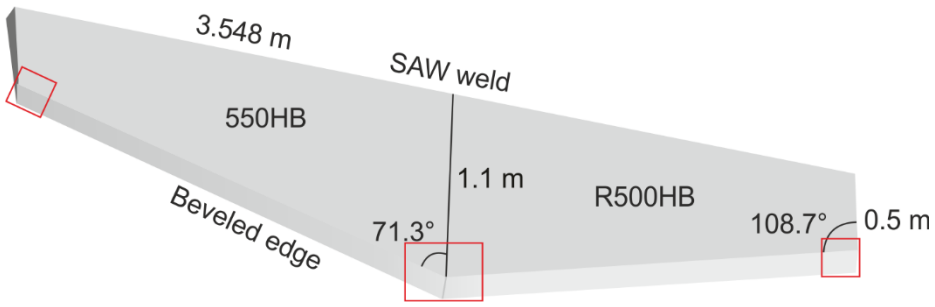

Fig. 2. Schematic of the studied in-service cutting edge. The red squares show the locations of characterized areas.

A high-speed slurry-pot with a dry abrasive bed (dry-pot) was used in the tests to simulate the in-service wear behavior of the cutting edge of the mining loader in a laboratory scale. The test system has been described in details elsewhere [17,22]. The cutting edge profiled samples were attached to the second sample holder level in the rotating shaft, as shown in Fig. 3. The total wear area was about 5000 mm^2. Two samples were rotated inside the gravel bed simultaneously. The tests were done in two parts so that the abrasive and the position of the samples were changed in the middle of the tests.

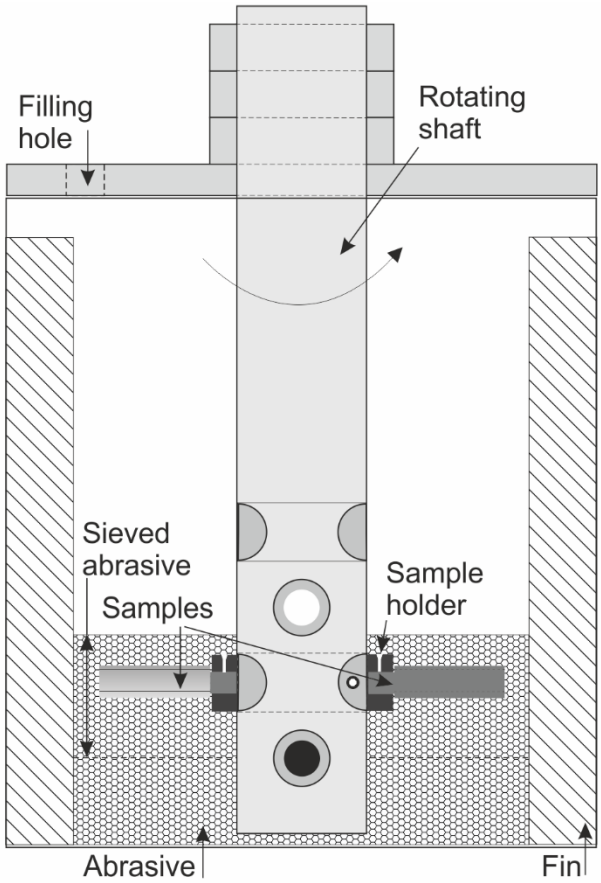

a)

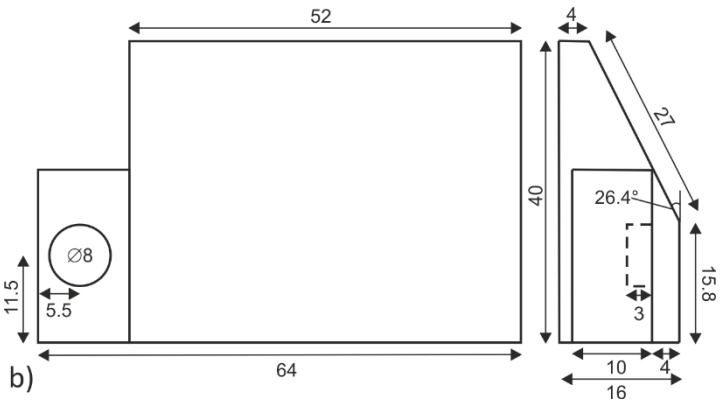

c)

Fig. 3. The test setup: a) schematic image of the test chamber, b) drawing of the sample, and c) photograph of the attached samples after the dry-pot wear test.

All steels were tested with quartzite and Kuru granite for 60 minutes at 500 rpm. In these tests, R500HB was the reference sample material. In addition, a comparison of the four abrasives was made using 240 minute tests at 250 rpm for two types of steel pairs: i) R500HB and 550HB as used in the in-service cutting edge and ii) 500HB and 600HB. The rotation speeds of 250 rpm and 500 rpm correspond to 2.5 m/s and 5 m/s in the edge of the sample, respectively. The travel distance of the sample edge during the test was doubled from about 18000 meters to 36000 meters, when the test time was increased from 60 min to 240 min and the test speed was decreased from 500 rpm to 250 rpm.

The amount of 8-10 mm size gravel in one test cycle was 9 kg for quartzite and granites. The amount of chromite, however, was 13.8 kg because the density of chromite is higher than that of the other used abrasives. Thus, the volume of rock was similar in each test, covering the samples as illustrated in Fig 3a.

Both the laboratory test samples and the in-service cutting edge of the loader bucket were thoroughly characterized. The wear surfaces were studied using Zeiss ULTRAplus field emission gun scanning electron microscope (FEG-SEM) and Alicona InfiniteFocus G5 3D measurement system. The cross-sections were characterized with FEG-SEM and an optical microscope, and the subsurface microhardness testing was performed with Matsuzawa MMT-X7 using a 50 g load (490.3 mN). The composition of the rocks was analyzed by Panalytical Empyrean Multipurpose Diffractometer (XRD). The abrasiveness and crushability of the abrasives were measured using a LCPC abrasimeter [2] at Metso Minerals. The bulk hardness values were determined from the cross-sections with Struers Duramin-A300 Vickers hardness tester using a 10 kg load.

3. Results

3.1. In-service case results

For the in-service testing, the cutting edge was constructed from R500HB and 550HB steels by submerged arc welding. The cutting edge was tested in CAT R2900G Underground Mining Load-Haul-Dumper (LHD), which is seen in operation in Fig. 4. For this dumper, the typical change interval of the cutting edge was about 1000 hours.

After 150 hours of operation, several cracks appeared near the installation welds on the side of the 550HB steel, next to the bucket-side shroud weld and the weld between the cutting edge and the bucket. The cracks were visible only in the 550HB steel and not in the weld nor in the R500HB steel. The welder repaired the first cracks in the side shrouds, but new cracks appeared in the 550HB plate at the corner. These cracks were so deep that repairing of them was not reasonable. Consequently, the in-service test was terminated after 217 hours of operation.

Fig 4. CAT R2900G LHD working on typical size of rocks. For reference, the diameter of the LHD tires is about 2 m.

Figures 5-7 show the wear profiles of the cutting edge measured by ATOS 3D-scanning, illustrating the effect of wear. The dark color in Figures 6-7 shows the original size of the cutting edge, which was later cut smaller from the sides due to a change to a smaller bucket finally used in the mine. The wear rate was highest on the underside of the cutting edge. Thus, the rocks under the cutting edge combined with the force of the machine pressing the cutting edge to the ground are much more abrasive than the rocks flowing inside the bucket. The centerline of the cutting edge is abraded more than the base steels because of the weld. The mass loss of R500HB was 54.95 kg and that of 550HB 40.51 kg, when determined by ATOS 3D-scanning. Thus, the harder 550HB was in these high-stress abrasive conditions significantly more wear resistant than R500HB.

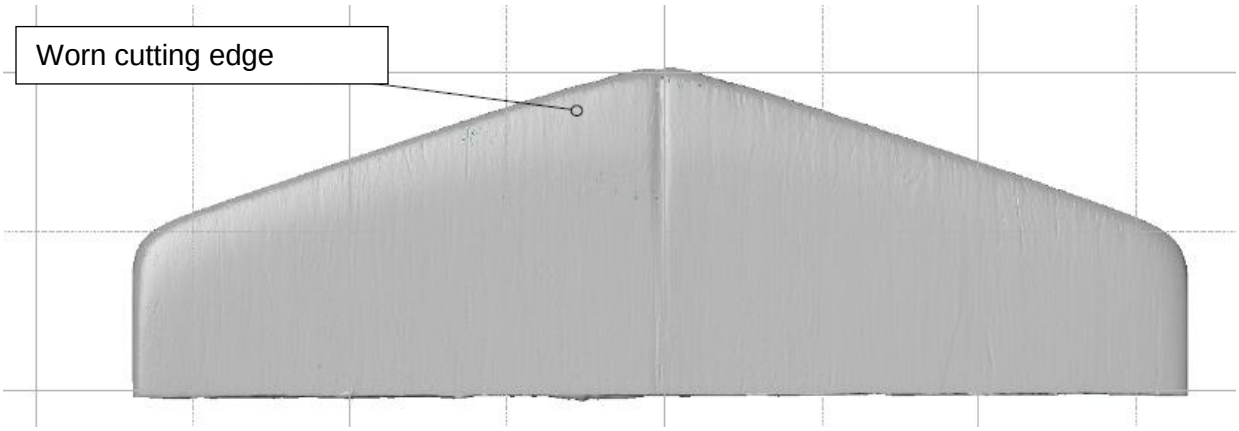

Fig 5. Underside of the cutting edge after 217 h of operation (550HB on the left).

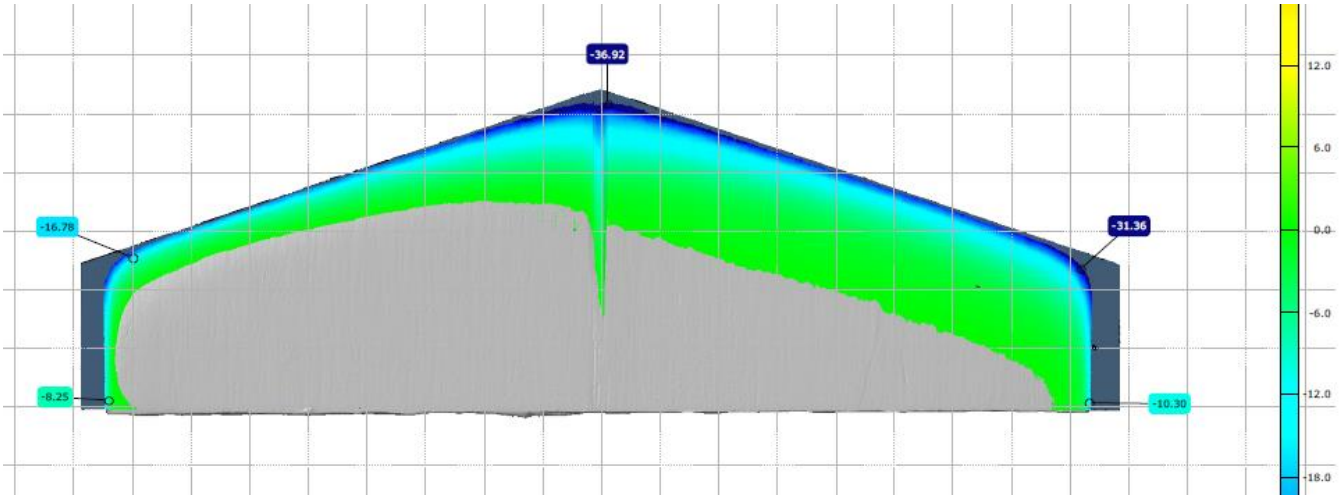

Fig 6. Wear profile of the underside of the cutting edge (550HB on the left).

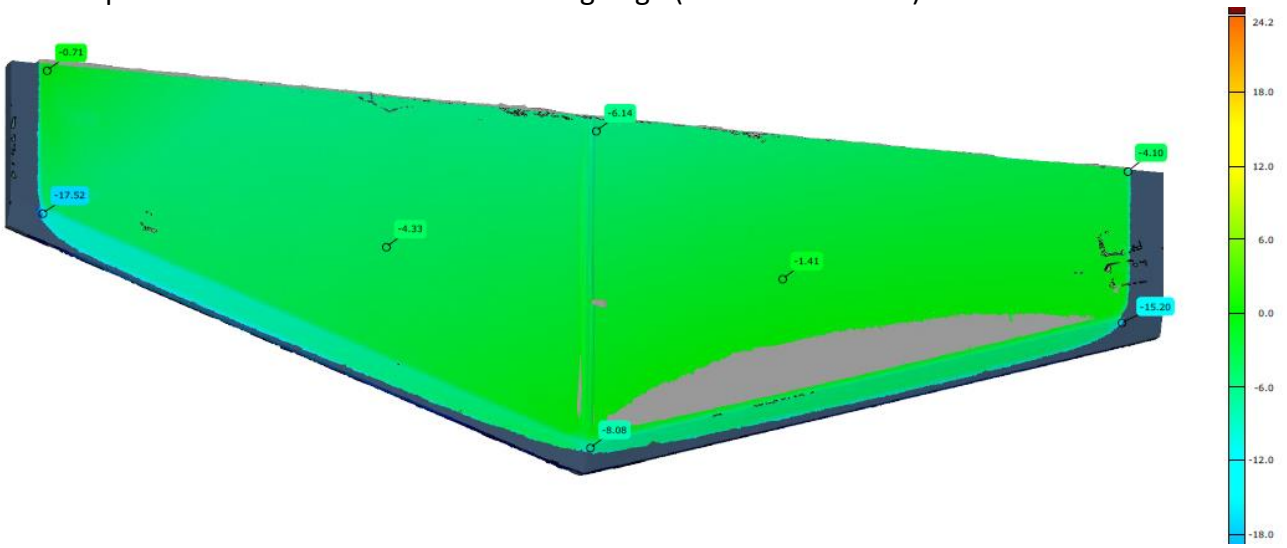

Fig 7. Wear profile of the upper side of the cutting edge (550HB on the left).

3.2. Laboratory wear test results

The first laboratory wear test series compared the high-stress abrasion of the wear resistant steels with quartzite and Kuru granite at 500 rpm test speed. Fig. 8a presents the mass loss results of the 60 minute tests. In these tests, quartzite was clearly more abrasive than Kuru granite, producing 33%-43% higher wear rates. However, the wear rates of the studied steels were not completely arranged by their hardness. For example, although the R500HB steel is harder than the 450HB and 500HB steels, it shows similar or higher mass loss. On the other hand, Fig. 8b shows that when the results are normalized using the reference sample, the R500HB steel exhibits a lower wear rate than the 450HB steel. Moreover, the 500HB steel performed better that its bulk hardness value gives reason to expect. Fig. 9b also indicates that the differences between the steels are more evident when granite is used as an abrasive, even though quartzite is more abrasive of these two.

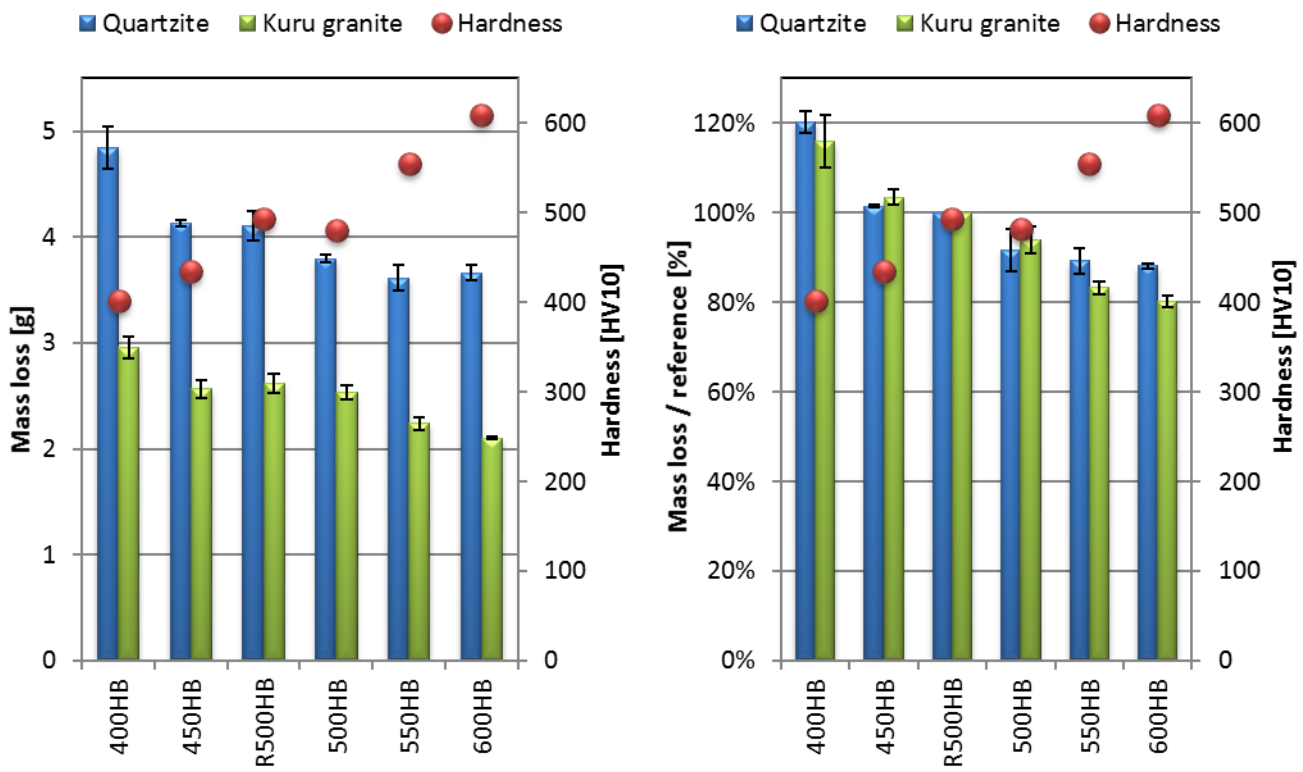

a) b)

Fig. 8. Test results with quartzite and Kuru granite for 60 minutes at 500 rpm showing a) absolute average mass loss and b) mass loss relative to the wear of the R500HB reference sample. The error bars represent the standard deviation.

The effect of abrasives on the wear of steels was further studied with four abrasives using samples made of the four hardest steels included in this study. The test speed was 250 rpm and the test time 240 min. Fig. 9 presents the results of the 240 minute tests for one sample per material without a reference sample. The R500HB samples were tested with the 550HB samples and the 500HB samples with the 600HB samples. Once again, quartzite produced the highest mass losses, but chromite and both granites produced larger differences between the steel grades compared to quartzite. Even though the travel distance of the sample edge during the tests was doubled from 18 km to 36 km meters, the wear rates were lower in the 250rpm/240 min tests than in the 500 rpm/60 min tests.

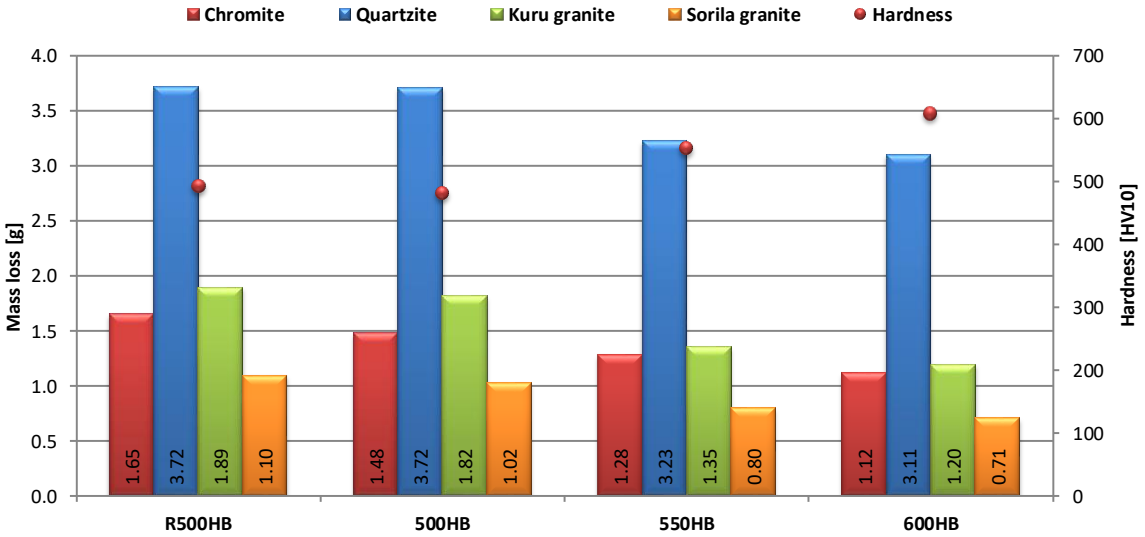

Fig. 9. Mass loss of the samples tested with four minerals for 240 minutes at 250 rpm.

During the tests, the gravel comminutes and the smaller rocks flow down and consolidate as a dense layer in the bottom of the chamber. Thus, the samples rotate inside the largest available freely flowing rock bed. The effect of the comminution of abrasives on the wear test results was studied by sieving the loose abrasives after the test cycles. Thus, Fig. 10 presents the effective rock size distribution causing wear in the samples until the end of the test. The downside of this sampling method, however, is that the finest fractions become underrepresented in the shown size distributions. In the 500 rpm/60 min tests, the abrasives were crushed clearly more than in the 250 rpm/240 min tests; less than 50% of the abrasives were in the initial 8-10 mm size range. The chromite comminuted radically more than the other studied abrasives, containing more than 40% of fine particles under 2 mm in size after the tests.

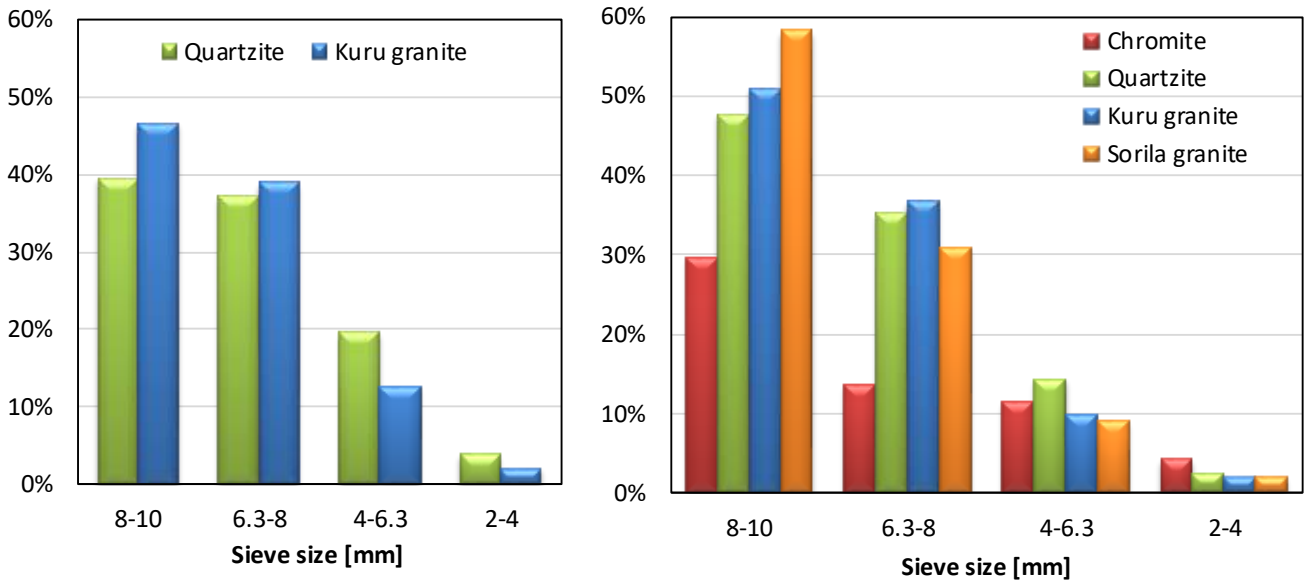

a) b)

Fig. 10. The sieved fractions of the abrasives taken from the area indicated in Fig. 3a after the test: a) 60 min at 500 rpm and b) 240 min at 250 rpm.

3.3. Surface characterization

The wear surfaces were characterized to study the effect of the steel hardness and the abrasives on the wear mechanisms. In all following wear surface images, the sample tip is on the right, i.e. the movement of the rock has been from the right to the left. The images are combined secondary electron and backscattered electron images (50:50) taken with a secondary electron detector SE2 and an angle selective backscattered electron detector AsB, respectively. The embedded rock shows dark grey on the lighter grey steel surface.

The pieces for the characterization of the in-service samples were cut from the middle and both ends of the tip of the cutting edge as marked in Fig. 2. Fig. 11 presents some examples of the characterized wear surfaces of the in-service cutting edge steels R500HB and 550HB. The surfaces show marks of cutting and surface fatigue by repeated ploughing. The scratches are long and deep and visibly deeper on the underside of the cutting edge. Quite high amount of rock was embedded in the steel surfaces, especially on the underside of the cutting edge. The reason for this difference in the embedment is that during loading the underside of the bucket ploughs heavily the ground and the rock pile, while on the upper side of the bucket the rocks have more possibilities to roll and thus cause less wear.

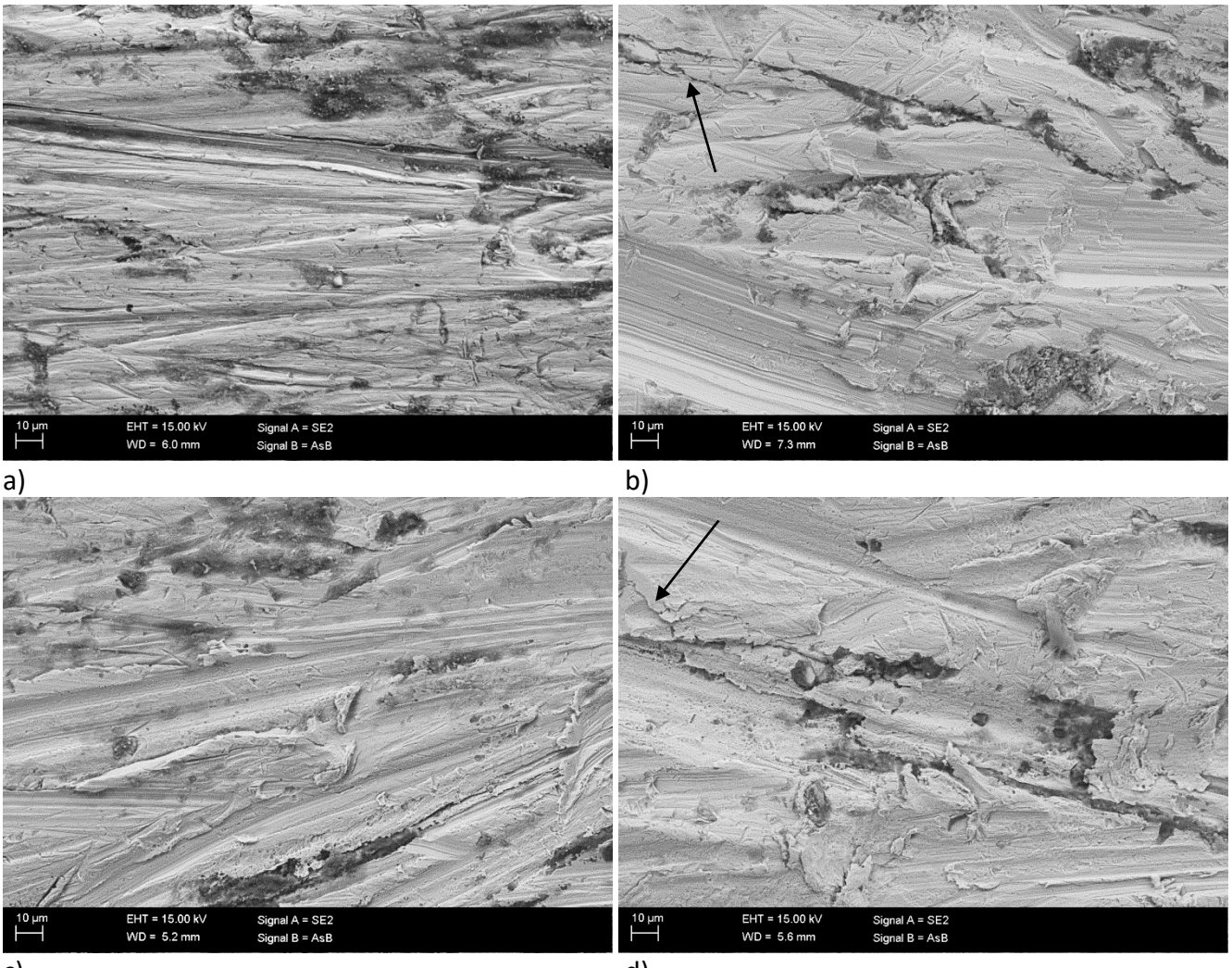

Fig 11. FEG-SEM images of the wear surfaces of R500HB (a and b) and 550HB cutting edges (c and d):

a and c are from the underside and b and d from the upper side of the cutting edge. The arrows indicate cracks on the surface.

The increase in steel hardness can be seen as decreased surface deformation of the wear surfaces. The scratches were visibly deepest in the softer 400HB steel. Moreover, the embedment of the rock on the surface was lowest in the 600HB steel. Fig. 12 shows SEM images of the wear surfaces tested for 60 minutes at 500 rpm with Kuru granite. All wear surfaces showed marks of heavy plastic deformation produced by ploughing of the rocks under the test samples. The sharp corners of the crushed minerals formed also micro cutting marks on the surfaces. However, in the present tests the micro fatigue appears to be the most destructive wear mechanism typical to high-stress abrasive wear with natural minerals [23]. In this wear mode, the rocks are ploughing the deformed steel surfaces repeatedly causing eventually material removal. Fig. 12a shows a good example of the cracked and partly detached deformed layer of mixed rock and steel.

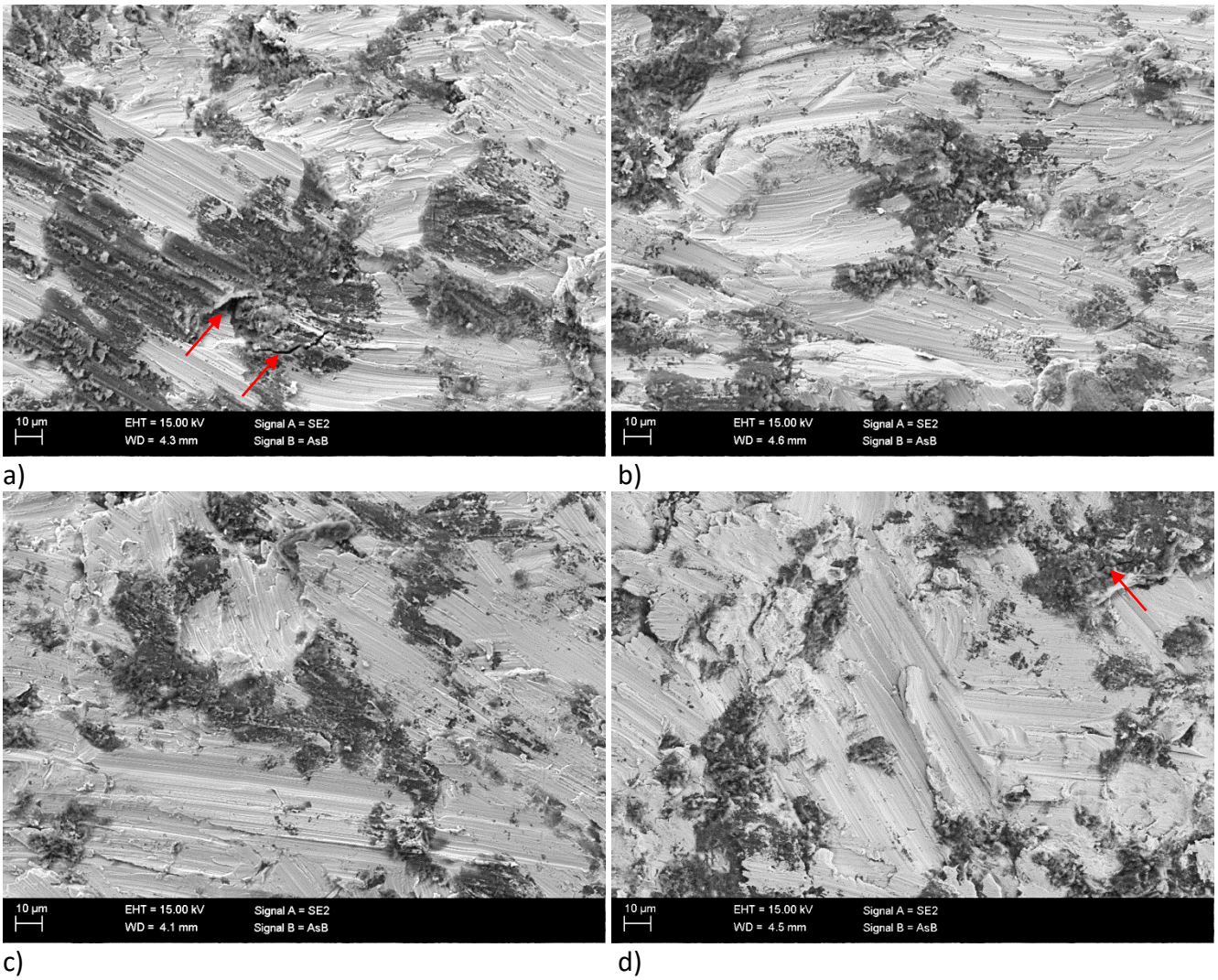

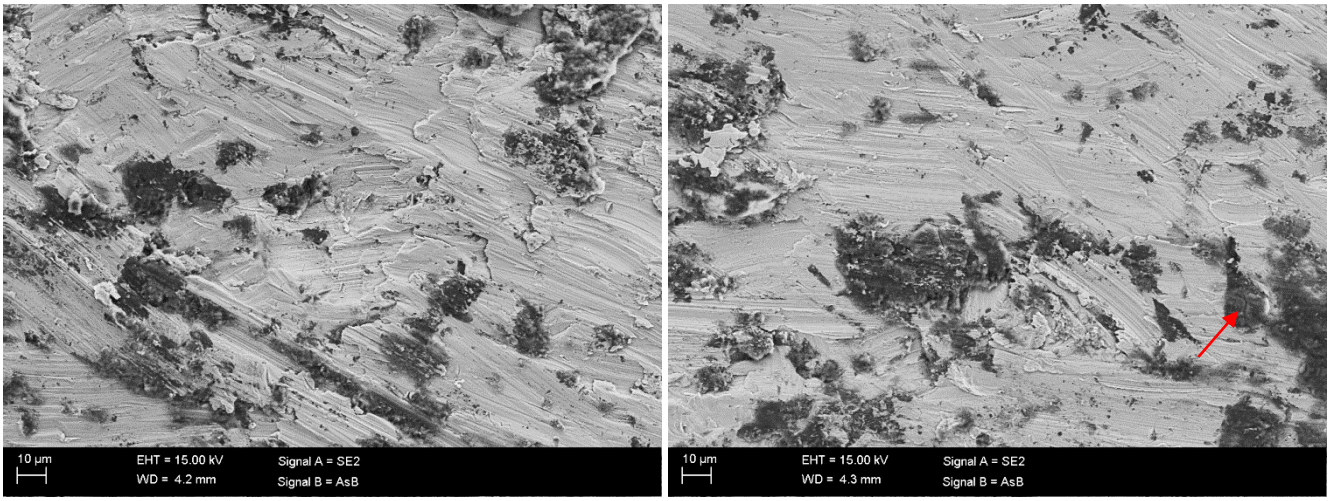

e) f)

Fig. 12. FEG-SEM images of the underside wear surfaces tested for 60 minutes at 500 rpm with Kuru granite a) 400HB, b) 450HB, c) R500HB, d) 500HB, e) 550HB, and f) 600HB. The arrows indicate cracks in the mixed rock and steel layer.

The effect of abrasive type on the wear mechanism was greater than the effect of the steel grade. Fig. 13 presents the wear surfaces of R500HB tested for 240 minutes at 250 rpm using chromite, quartzite, Kuru granite, and Sorila granite. The chromite tested surfaces show the deepest and longest cutting marks and also well defined ridges from ploughing. The scratches are much finer in the quartzite tested surfaces. Moreover, the embedded rock is very fine and scattered as thin particles on the wear surface. The embedded granite formed thick blocks on the wear surfaces, which are clearly thickest when using Sorila granite. The granite particles also tend to round during the long test cycle, and as a consequence, rolling marks were observed on the wear surfaces.

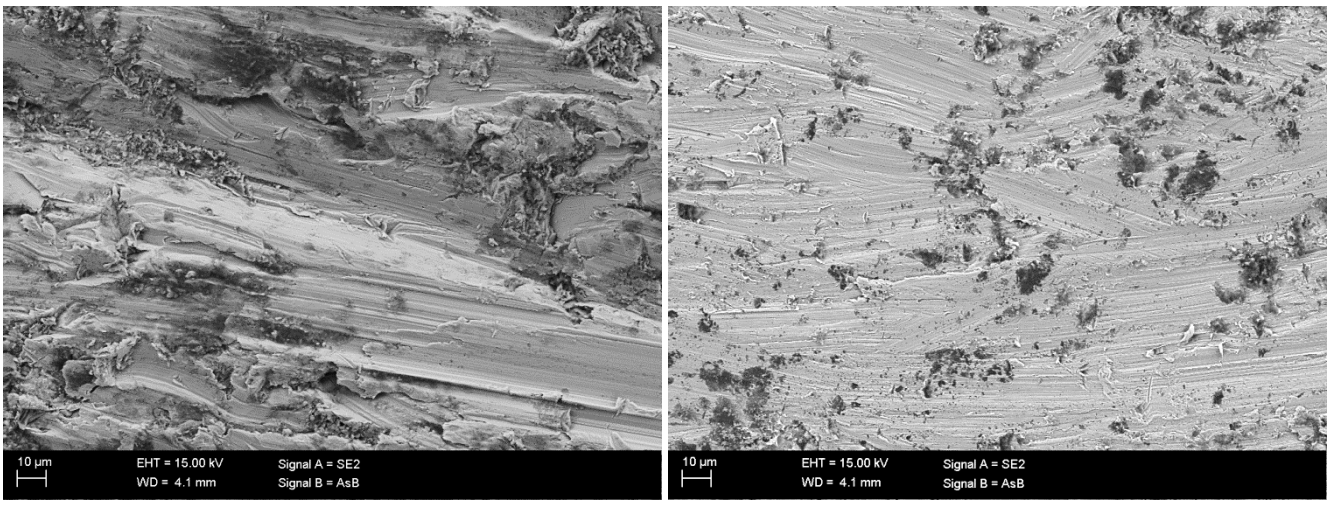

a) b)

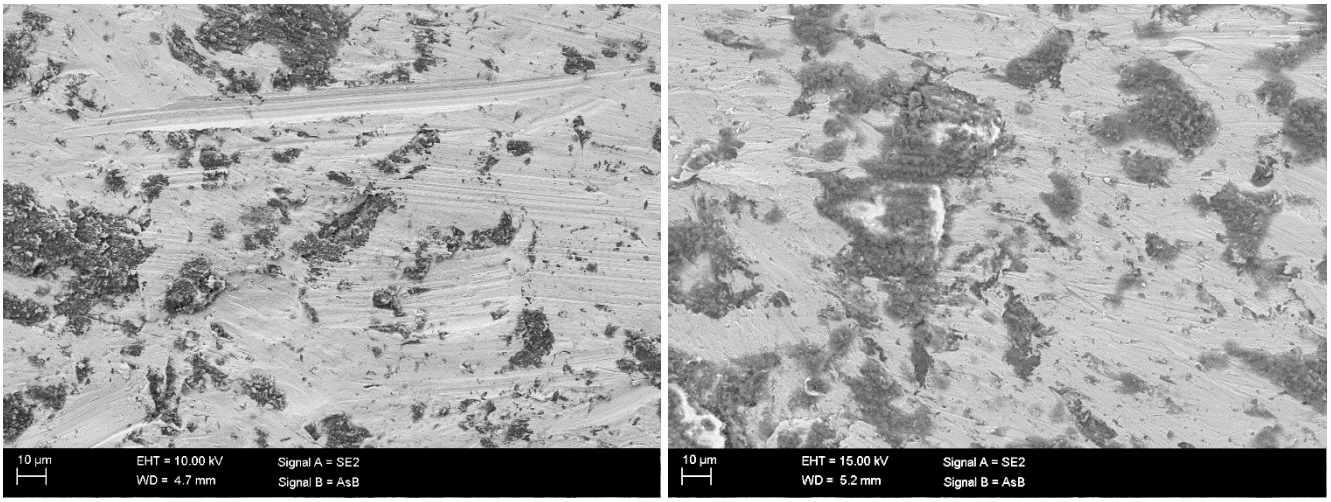

c) d)

Fig. 13. FEG-SEM images of the underside wear surfaces of the R500HB samples tested for 240 minutes at 250 rpm with a) chromite, b) quartzite, c) Kuru granite, and d) Sorila granite.

Although the appearance of the in-service and laboratory tested wear surfaces were similar in the micro scale, in a larger scale the effect of much larger rocks causing wear in the mining conditions was clearly visible. Fig. 14 presents 3D profilometer images of R500HB tested in laboratory with chromite and in the in-service conditions. Even in a few square millimeter area, the surface roughness values of the in-service wear surface are clearly higher.

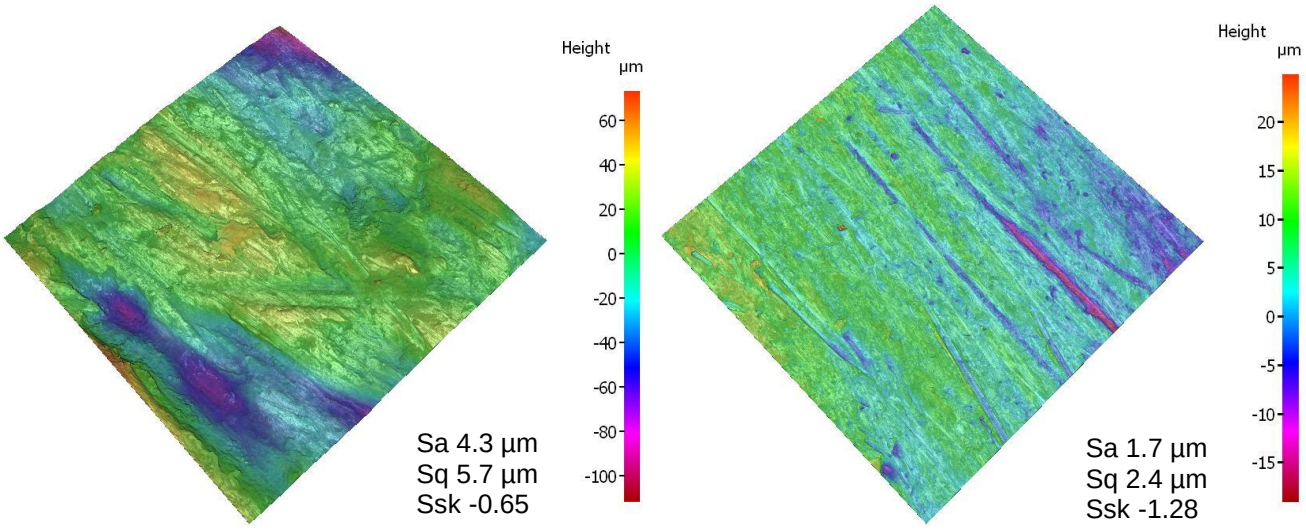

a) b)

Fig. 14. 3D profilometer images of the R500HB steel surfaces tested a) in the in-service conditions and b) in a laboratory for 240 minutes at 250 rpm in chromite. Image area is 3 mm x 3 mm.

3.4. Cross-section analysis

The cross-section analysis was made to study the deformation and work hardening of the subsurface layers of the steels by microscopy and micro hardness testing. Tens of micrometers thick and partially cracked white layers were observed in the cross-sections of the in-service samples. The white layers were thickest, up to 150 µm on the underside of the cutting edge, where the hardness of the layers was on average 740±25 HV0.05 for both steels. However, even values up to 790 HV0.05 were

measured in some locations, where two or more white layers were overlapping. On the upper side of the cutting edges, the thickness of the white layers was typically below 50 µm. Fig. 15 presents examples of the thickness and hardness profiles of the white layers. The high hardness of the white layers explains the brittle nature of the fractures. Fig. 16 shows an example of cracking along the white layers. The cracks stop at the deformed layer below the white layer, i.e. so-called dark layer. In the R500HB steel, the hardness values in this layer were as low as 390 HV0.05. The tilted view in Fig. 16b shows also the appearance of the wear surface above the white layer, where abrasive particles have been trapped under the heavily deformed and cracked lip.

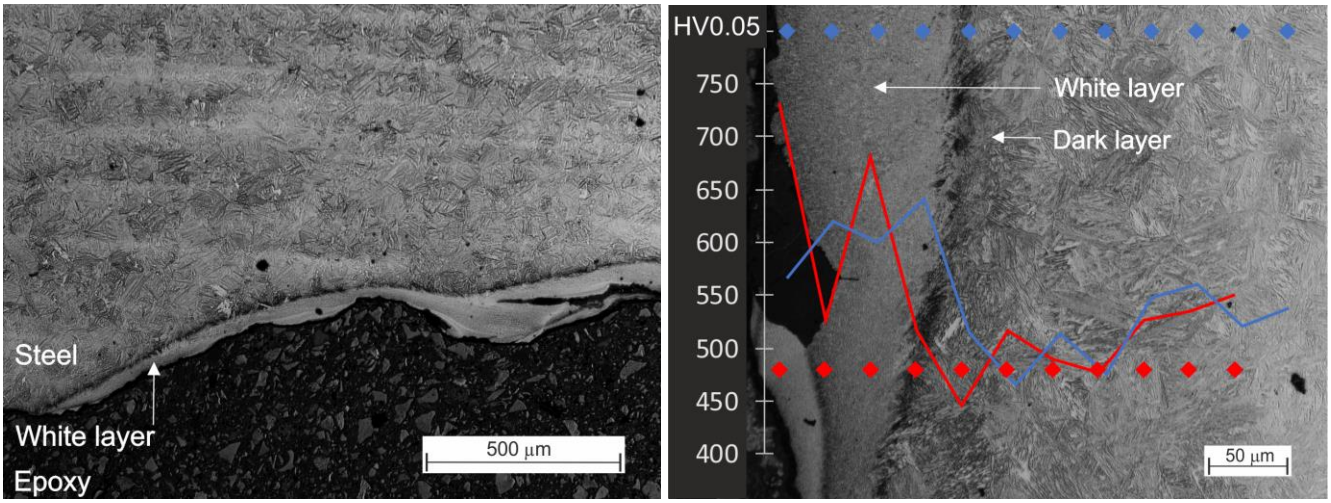

a) b)

Fig. 15. Optical micrographs from the cross-section of the underside of the in-service R500HB sample showing thick white layers. The hardness profiles (b) were measured from the diamond marker locations.

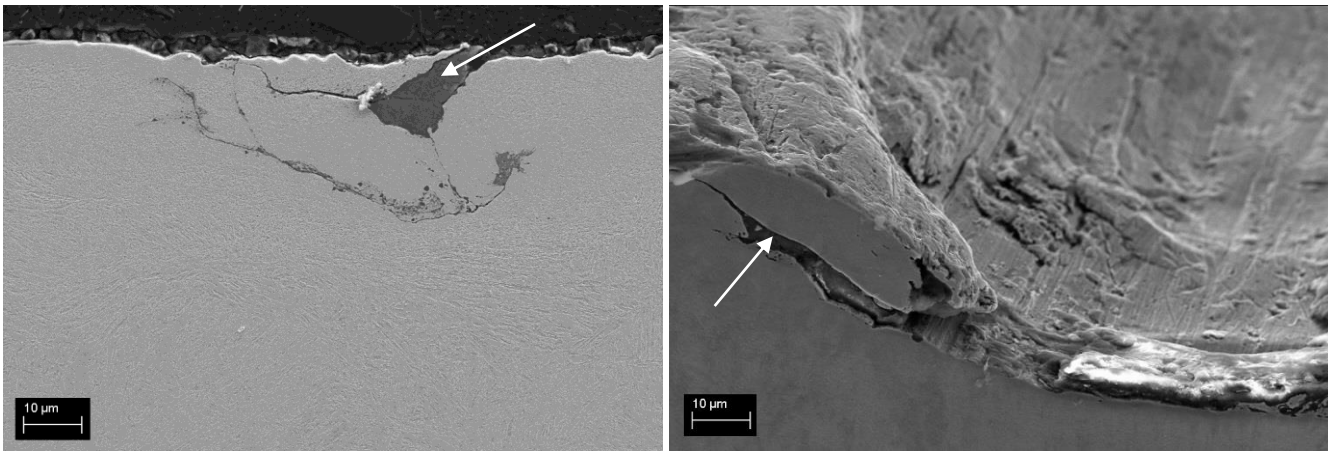

a) b)

Fig. 16. Cross-section FEG-SEM images of white layers in the 550HB in-service sample. The arrows mark embedded rock particles.

Figure 17 shows the thin, less than 10 µm thick white layers that were occasionally formed in all laboratory samples. They were found especially in the bottom of deep scratches. The white layers were typically thickest at the highly rounded outer corners of the samples. Moreover, continuous white layers were formed in the outer edge of the samples, where the sample velocities were the

highest. Fig. 17d shows delamination of the white layer from the outer edge of the 500HB sample. In the 550HB sample (Fig. 17e), it looks like the white layer has already delaminated and the deformed layer is going to crack. Although the deformed layers were deepest in the 400HB steel, only a couple of micrometers thick white layers were observed in this material.

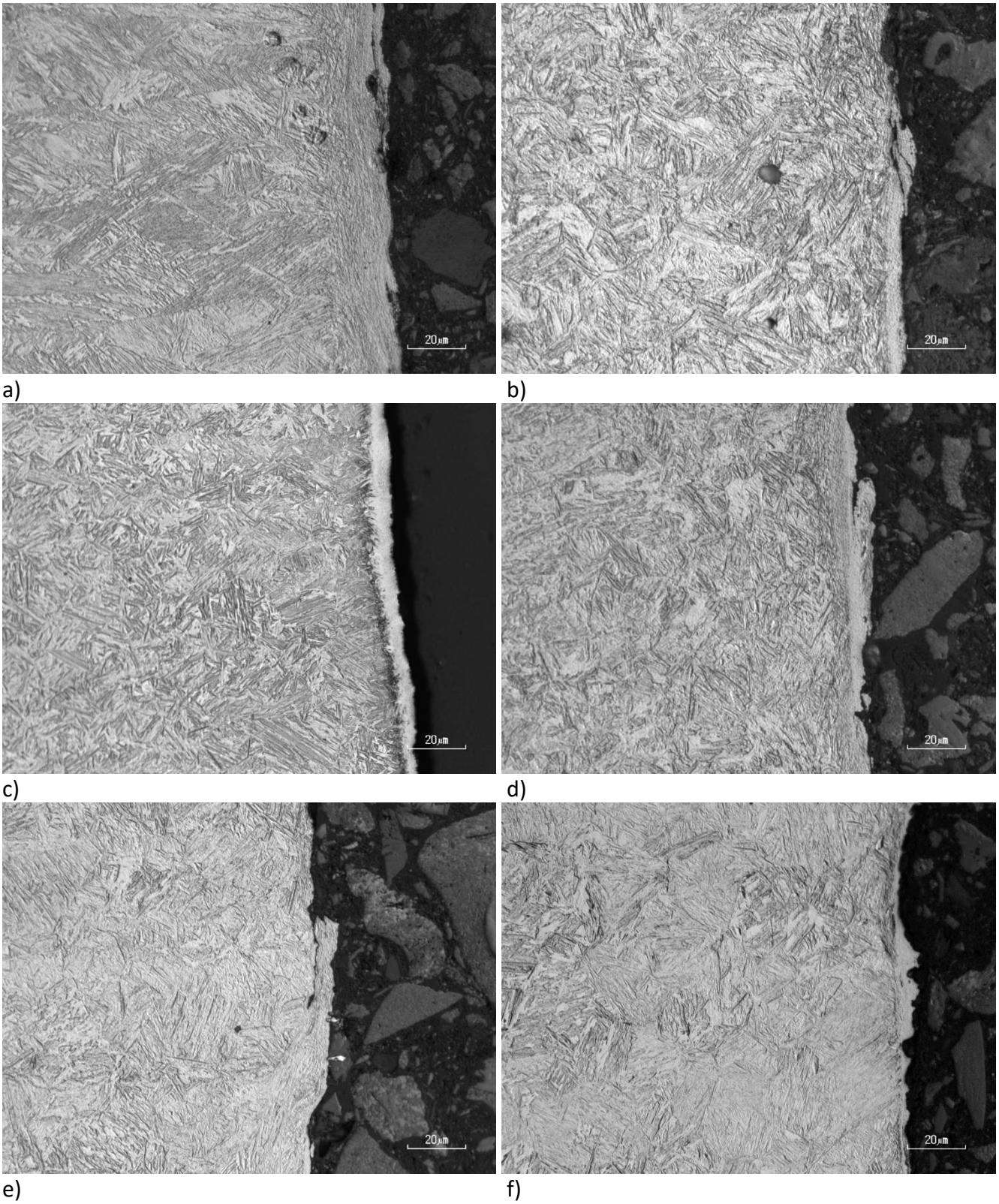

a) b)

c) d)

e) f)

Fig. 17. Optical micrographs of the cross-sections of the outer edges of the samples tested for 60 minutes at 500 rpm with quartzite a) 400HB, b) 450HB, c) R500HB, d) 500HB, e) 550HB, and f) 600HB.

In the 250 rpm/240 min tests, the formed white layers were thicker, up to 25 µm and less cracked when compared to the 500 rpm/60 min tests. The hardness of the white layers was up to 800 HV; similar to the in-service cases. It should be noted that the hardness of the white layers in the 600HB steel was at the same level with the 500-550 grade steels. The white layers were thinnest, less than 5 µm, in the chromite tested samples and thickest, even as thick as 25 µm, in the quartzite tested samples. Fig. 18 shows a couple of examples of the white layers formed in the 250 rpm/240 min tests. In general, the harder the steel, the thicker the formed white layers are.

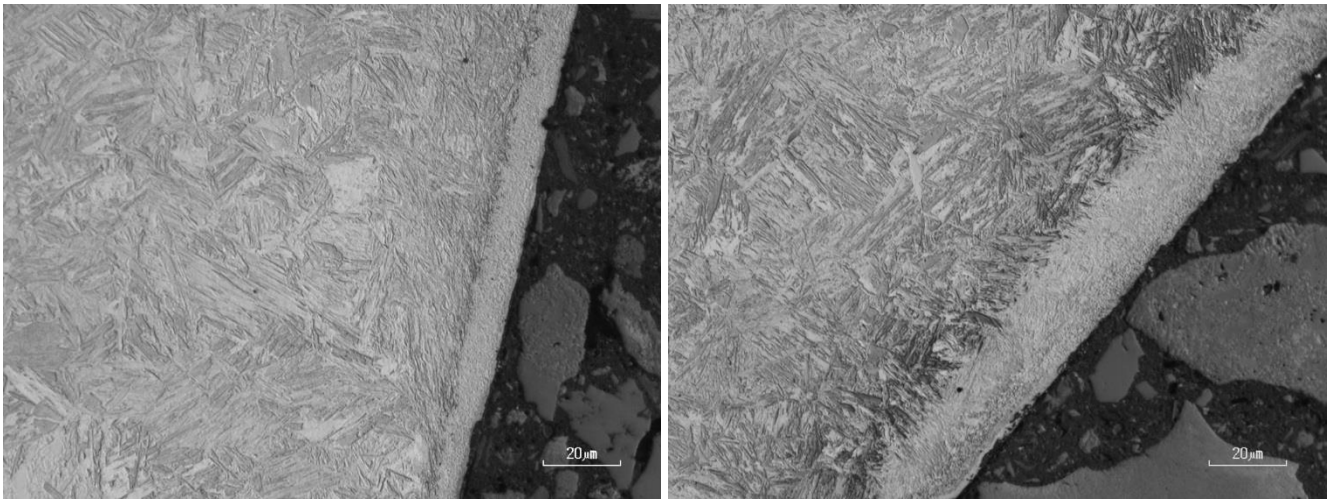

a) b)

Fig. 18. Optical micrographs of the cross-sections of a) 500HB and b) 600HB samples tested for 240 minutes with quartzite at 250 rpm.

4. Discussion

Although the size of the loaded rocks in a mine can be really big, the true local contact areas between the rocks and the steel surfaces are similar as in the laboratory tests. Accordingly, the width of the scratches on the sample surfaces were quite similar in both cases. However, only the small and hard particles in the chromite ore produced similar long and well-defined scratches in the laboratory tests as found in the in-service samples. Granite and quartzite particles, on the other hand, rounded during the tests and thus partially rolled over the sample surface.

In the laboratory wear tests, quartzite produced the highest wear rates at both test speeds and tests times. In the 500 rpm tests, quartzite produced up to 74 % higher mass losses than granite in 60 minutes, and in the 250 rpm tests up to 178 % higher mass losses than chromite in 240 minutes. Despite the high wear rates produced by quartzite, the tests with Kuru granite showed the biggest differences between the wear rates of the studied steels. Fig. 19 shows how much lower the wear rates of the 550HB steel samples were when compared to the R500HB samples. In the 250 rpm/240 min tests, the difference between the steels was quite similar as in the in-service case, when the abrasive was granite or chromite. The difference was much smaller when the abrasive was quartzite

or the speed was higher. In abrasive wear, quartzite forms a thin in-situ composite layer with steel, which has been observed to have an effect on the wear behavior of the steels [24].

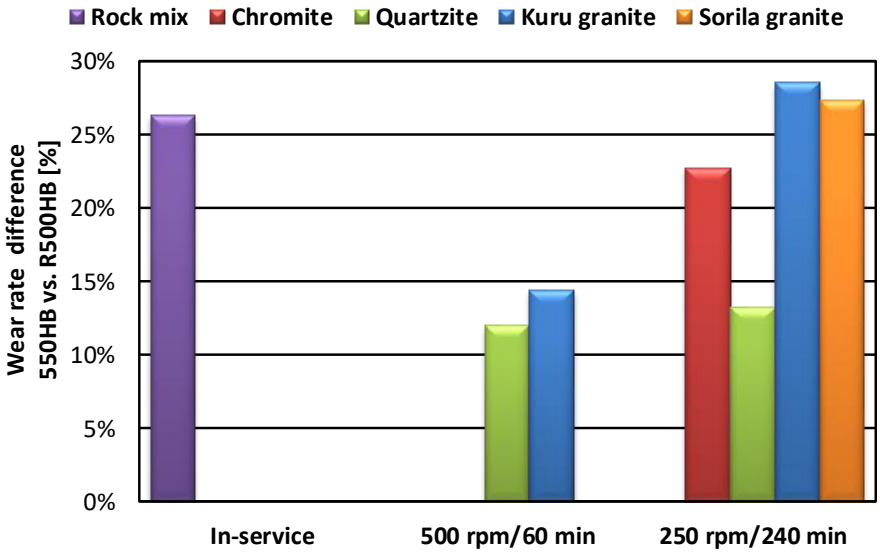

Fig. 19. Reduction of the wear rate when R500HB is replaced by 550HB in the in-service conditions and in the laboratory tests with different abrasives and test conditions.

Fig. 20 presents the wear rates of the R500HB and 550HB steels in mm/h obtained by dividing the determined mass loss by the test time, the initial contact area, and the density. For the in-service samples, the actual contact time with gravel was estimated to be about 25% of the total operation time based on the loading videos taken during the operation in the mine. However, it is only a rough estimate because the loading types changed during the operation of the loader. In the 500 rpm/60 min tests with Kuru granite, the wear rate is in the same level as in the mining conditions with various rock types. Although the travel distance of the sample tip was doubled in the 250 rpm/240 min tests compared to the 500 rpm/60 min tests, the wear rate was much higher in the 500 rpm tests. For example, the wear rates of the 550HB steel were 350 % higher with quartzite and as much as 560 % higher with Kuru granite than in the 250 rpm/240 min tests. This clearly indicates changes in the wear mechanism: for example, the higher rotation speed of the sample produces higher energy impacts, which will remove material more effectively by means of micro fatigue.

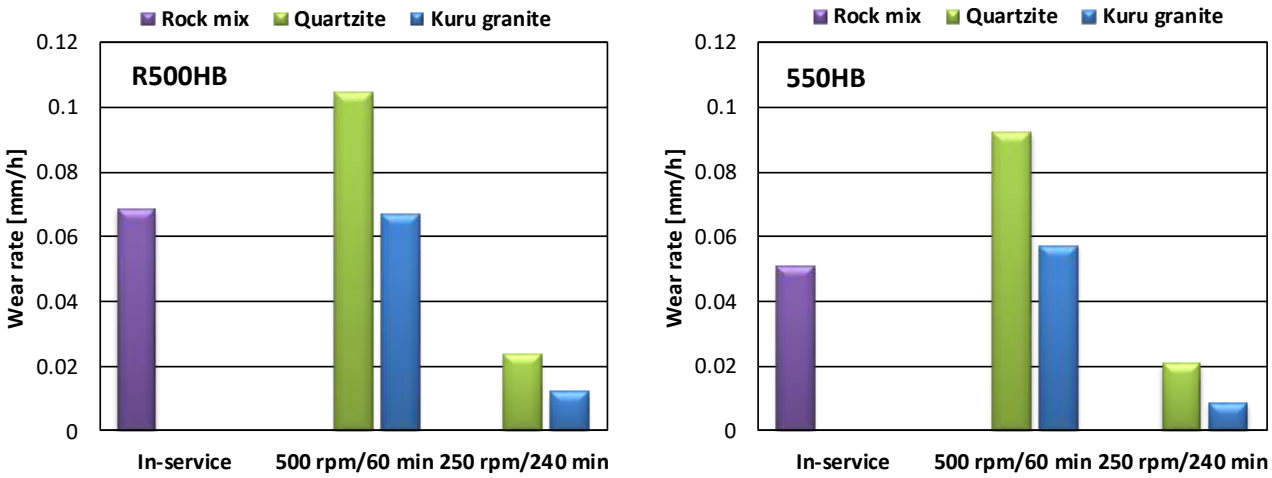

Fig. 20. Wear rates of the R500HB and 550HB steels in the used test environment.

In all laboratory tests, the white layers were formed in the bottom of the scratches and especially on the outer edge and tip of the samples. In the in-service samples, the white layers were thicker (up to 150 µm) than in the laboratory samples (up to 25 µm), but similar failure mechanisms were observed. When the deformability of the hard white layers was exceeded, they cracked and failed. Especially in the 500 rpm/60 min tests, the white layers were cracked and failed in a similar manner as in the in-service case. In the 250 rpm/240 min tests, the formed white layers were 10-20 µm thicker and more intact than in the tests with the higher speed. This indicates that the formation of white layers may protect the steels in milder wear conditions, but at higher speeds and loads they tend to fail, which may even accelerate wear in certain conditions. This is in agreement with the studies of Yang et al. [25,26], who also stated that depending on the direction of the crack propagation, the white layers fail either by delamination or spalling.

The laboratory tests were found to produce white layers and wear surfaces that remind more the upper side of the cutting edge than its more heavily worn underside. Thus, the dry-pot laboratory tests model better the penetration of the cutting edge into the rock pile and sliding of the rock against the upper side of the cutting edge. However, an obvious limitation of the current test system is that there is no vertical compressive force acting on the cutting edge, i.e. the mass of the rock pile and the weight of the loader, as explained in the Introduction.

When there are only small differences observed in the test results, such as in the cases of 450HB and R500HB or 550HB and 600HB, the use of a reference sample is very important, as it reduces the effect of differences between the batches of natural abrasives. On the other hand, the standard deviations in the wear rates of the reference samples were only 3.4% with quartzite and 3.7% with granite, which are reasonably good values for this type of wear test.

The dry-pot test procedure is quite similar to the LCPC abrasiveness tests; two steel impellers are rotating in a pot filled with gravel. The LCPC test gives 40 % higher abrasiveness values for quartzite than for Kuru granite, while the dry-pot test produced 50-75 % higher mass losses with quartzite. Moreover, the dry-pot test gives Sorila granite higher abrasiveness than for Kuru granite and chromite. The difference is marked with chromite, the abrasiveness of which is only one third of that

of Sorila granite. However, in the dry-pot test both Kuru granite and chromite produced higher wear rates compared to Sorila granite. This indicates a marked difference in the wear processes between the LCPC and dry-pot tests. The high energy impacts during the LCPC test break the rock more efficiently. Moreover, the test is much shorter (5 min) and practically covers only the running-in phase of the steel impeller. These results indicate that in the estimation of the abrasivity of the rock in a certain application, the entire wear environment should be taken into consideration and that the simplified abrasivity tests may give incorrect estimations, since they are practically based on measuring the strength of the rock materials. Moreover, the steel grades used in the abrasivity tests have typically very different mechanical properties compared to the ones used in the actual conditions in the field. Moreover, the contact conditions and tests speeds do not match with the in-service conditions either. Based on the presented results and observations, it can be concluded that the dry-pot test method could be suitable also for abrasivity testing for selected mining applications, such as loader buckets, feed hoppers, and screens.

A great advantage of this study was the possibility to characterize two materials that had been used in a chromite mine, and to compare them with laboratory wear tested samples. During two years of recording, the replacement frequency of the cutting edges of the selected LHD loader varied from 447 hours to 1588 hours. Thus, the 217 hour in-service test was much shorter than the average 1041 hours between the replacements. The SAW weld connecting the two test steels was of high-quality, but the MIG/MAG installation weld of the 550HB steel failed due to hydrogen embrittlement. Apparently the preheating of the hard steel was made at a too low temperature and the installation welding wire was not good enough for this kind of a hard steel. This is an example of the challenges that are often encountered when new materials are introduced to the in-service use, or when material testing is made in the in-service conditions. However, the wear rates were high enough to produce a clear difference between the two steels used in the test cutting edge. Moreover, the laboratory wear test results support the in-service case results. When the welding parameters are optimized, it is quite realistic to expect an over 25% increase in the lifetime of the cutting edges, if the material is changed from the current R500HB steel to 550HB steel.

5. Conclusions

In this study, the laboratory wear tests with six steel grades, four abrasives, and two testing procedures were conducted. Two of the steels were tested also as cutting edges of the loader bucket in real mining conditions. Based on the analysis of the laboratory and the in-service wear test results and the characterization of the wear surfaces and microstructures, the following conclusions can be drawn:

- The laboratory wear test results are in accordance with the in-service case results; an over 25% increase in the lifetime can be expected, when the current R500HB steel is changed to a harder 550HB steel.
- A low sample rotation speed with a long testing time and granite or chromite as an abrasive produce the highest wear rate differences between the steel grades, which is in accordance with the in-service results.
- When tested at the higher sample rotation speed with granite, the wear rates in the dry-pot tests were similar as in the in-service conditions.

- Although chromite produced similar wear surfaces as found in the in-service samples taken from a chromite mine, the formed white layers were not as thick, because the chromite ore comminuted heavily in the laboratory tests. Thus, granite seems to be the most suitable abrasive for wear testing in this kind of application in the Finnish bedrock.
- The dry-pot tests produce repeatable results with a quite small standard deviation in the mass loss values.
- The dry-pot wear tester is also suitable for determining the abrasivity of rocks in certain mining applications.
- The formation of white layers increased the wear rate in the harder steel grades, when the wear mechanism was more of the impact-abrasive type.

Acknowledgements

This work was done within the DIMECC BSA (Breakthrough Steels and Applications) Programme as part of the DIMECC Breakthrough Materials Doctoral School. We gratefully acknowledge the financial support from the Finnish Funding Agency for Innovation (Tekes) and the participating companies. Pasi Lassuri and Jarmo Räsänen from Outokumpu Kemi Mine are thanked for enabling the testing in the mine. The authors also gratefully acknowledge Specialist Anu Kemppainen from SSAB Europe for her help and advices, and B.Sc. Verner Nurmi for his assistance with the wear tests and sample preparation.

References

[1] Tanttari M. Facing wear challenges in underground loaders. TWC Int. Wear Semin., 2009, p. 1–12.

[2] Abrasimeter. Paris, France: Matériales des Laboratoires des Ponts et Chaussées; 1985.

[3] Thuro K, Käsling H. Classification of the abrasiveness of soil and rock. Geomech Und Tunnelbau 2009;2:179–88. doi:10.1002/geot.200900012.

[4] Drucker P. Validity of the LCPC abrasivity coefficient through the example of a recent Danube gravel Aussagekraft des LCPC-Abrasivitätskoeffizienten am Beispiel eines rezenten Donauschotters. vol. 4, 2011, p. 681–91. doi:10.1002/geot.201100051.

[5] Küpferle J, Röttger A, Alber M, Theisen W. Assessment of the LCPC abrasiveness test from the view of material science / Bewertung des LCPC-Abrasivitätstests aus werkstofftechnischer Sicht. Geomech Tunn 2015;8:211–20. doi:10.1002/geot.201500002.

[6] Ko TY, Kim TK, Son Y, Jeon S. Effect of geomechanical properties on Cerchar Abrasivity Index (CAI) and its application to TBM tunnelling. Tunn Undergr Sp Technol 2016;57:99–111. doi:10.1016/j.tust.2016.02.006.

[7] Deliormanlı AH. Cerchar abrasivity index (CAI) and its relation to strength and abrasion test methods for marble stones. Constr Build Mater 2012;30:16–21. doi:10.1016/j.conbuildmat.2011.11.023.

[8] Nikas GK. Modeling Dark and White Layer Formation on Elastohydrodynamically Lubricated Steel Surfaces by Thermomechanical Indentation or Abrasion by Metallic Particles. J Tribol

2015;137:31504. doi:10.1115/1.4029944.

[9] Cho DH, Lee SA, Lee YZ. Mechanical properties and wear behavior of the white layer. Tribol. Lett., vol. 45, 2012, p. 123–9. doi:10.1007/s11249-011-9869-4.

[10] Hossain R, Pahlevani F, Witteveen E, Banerjee A, Joe B, Prusty BG, et al. Hybrid structure of white layer in high carbon steel - Formation mechanism and its properties. Sci Rep 2017;7:1–12. doi:10.1038/s41598-017-13749-7.

[11] Manco GL, Caruso S, Rotella G. FE modeling of microstructural changes in hard turning of AISI 52100 steel. Int J Mater Form 2010;3:447–50. doi:10.1007/s12289-010-0803-3.

[12] Mao C, Zhou Z, Zhang J, Huang X, Gu D. An experimental investigation of affected layers formed in grinding of AISI 52100 steel. Int J Adv Manuf Technol 2011;54:515–23. doi:10.1007/s00170-010-2965-z.

[13] Ji W, Shi J, Liu X, Wang L, Liang SY. A Novel Approach of Tool Wear Evaluation. J Manuf Sci Eng 2017;139:1–8. doi:10.1115/1.4037231.

[14] Attanasio A, Umbrello D, Cappellini C, Rotella G, M'Saoubi R. Tool wear effects on white and dark layer formation in hard turning of AISI 52100 steel. Wear 2012;286–287:98–107. doi:10.1016/j.wear.2011.07.001.

[15] Hosseini SB, Klement U, Yao Y, Ryttberg K. Formation mechanisms of white layers induced by hard turning of AISI 52100 steel. Acta Mater 2015;89. doi:10.1016/j.actamat.2015.01.075.

[16] Chen T, Qiu C, Liu X, Qian X, Liu G. Study on test method of white layer microhardness in hard cutting based on chord tangent method. Int J Adv Manuf Technol 2017:1–9. doi:10.1007/s00170-017-0197-1.

[17] Vuorinen E, Ojala N, Heino V, Rau C, Gahm C. Erosive and abrasive wear performance of carbide free bainitic steels - Comparison of field and laboratory experiments. Tribol Int 2016;98:108–15. doi:10.1016/j.triboint.2016.02.015.

[18] Vuorinen E, Heino V, Ojala N, Haiko O, Hedayati A. Erosive-abrasive wear behavior of carbide-free bainitic and boron steels compared in simulated field conditions. Proc Inst Mech Eng Part J J Eng Tribol 2017. doi:10.1177/1350650117739125.

[19] Valtonen K, Ratia V, Ojala N, Kuokkala V-T. Comparison of laboratory wear test results with the in-service performance of cutting edges of loader buckets. Wear 2017;388–389:93–100. doi:10.1016/j.wear.2017.06.005.

[20] Fourmeau M, Gomon D, Vacher R, Hokka M, Kane A, Kuokkala V-T. Application of DIC Technique for Studies of Kuru Granite Rock under Static and Dynamic Loading. Procedia Mater Sci 2014;3:691–7. doi:10.1016/j.mspro.2014.06.114.

[21] Ratia V, Heino V, Valtonen K, Vippola M, Kemppainen A, Siitonen P, et al. Effect of abrasive properties on the high-stress three-body abrasion of steels and hard metals. Finnish J Tribol 2014;32:3–18.

[22] Ojala N, Valtonen K, Kivikytö-Reponen P, Vuorinen P, Kuokkala V-T. High speed slurry-pot erosion wear testing with large abrasive particles. Finnish J Tribol 2015;33:36–44.

[23] Peng SG, Song RB, Sun T, Yang FQ, Deng P, Wu CJ. Surface failure behavior of 70Mn martensite

steel under abrasive impact wear. Wear 2016;362–363:129–34. doi:10.1016/j.wear.2016.05.019.

[24] Heino V, Valtonen K, Kivikytö-Reponen P, Siitonen P, Kuokkala VT. Characterization of the effects of embedded quartz layer on wear rates in abrasive wear. Wear 2013;308:174–9. doi:10.1016/j.wear.2013.06.019.

[25] Yang YY, Fang HS, Huang WG. A study on wear resistance of the white layer. Tribol Int 1996;29:425–8. doi:10.1016/0301-679X(95)00099-P.

[26] Yang Y-Y, Fang H-S, Zheng Y-K, Yang Z-G, Jiang Z-L. The failure models induced by white layers during impact wear. Wear 1995;185:17–22. doi:10.1016/0043-1648(94)06586-1.